Sub-100 ps monolithic diamond Raman laser emitting at 573 nm

Jari Nikkinen, Vasili Savitski, Sean Reilly, Łukasz Dziechciarczyk, Antti Härkönen, Alan Kemp and Mircea Guina

***Abstract*—We report a compact and efficient picosecond diamond Raman laser at 573 nm wavelength. The laser consists of a 0.5 mm thick single-crystal synthetic diamond coated to form a plane–plane laser resonator, and pumped at 532 nm by a frequency-doubled Q-switched microchip laser system. The pump delivers 85 ps pulses at 100 kHz repetition rate at a maximum average power of ~500 mW. We demonstrate 1st Stokes emission from the diamond Raman laser with maximum power of 175 mW, corresponding to a conversion efficiency of 47% and a pulse duration of 71 ps. Substantial pulse shortening is obtained by proper adjustment of the pump spot diameter on the diamond sample. A minimum pulse duration of 39 ps is reported for a conversion efficiency of 36% and 150 mW output power. The simplicity of the architecture makes the system highly appealing as a yellow picosecond laser source.**

***Index Terms*—Raman lasers, Diamond Raman lasers, Q-switched lasers, Pulsed lasers, Visible lasers.**

I. Introduction

APPLICATIONS in fluorescence lifetime imaging, two-photon microscopy and spectroscopy often require specialized excitation sources [1] with stringent requirements on wavelength and pulse duration. One method of accessing hard-to-reach wavelengths is to use ubiquitous solid-state sources to pump Raman lasers, with diamond being an excellent Raman laser material due to its unrivalled thermo-optic properties [2] and large Raman shift. The latter gives access to yellow-orange spectral range under green pumping, which is of interest in ophthalmology (retinal vascular disease, photocoagulation), astronomy (laser guide stars), and dermatology (vascular lesions, pigmentation, acne).

While Raman conversion of CW and Q-switched lasers has become routine [3–7], extending the wavelength coverage of ultrafast (pico- and femtosecond) sources is significantly more complex, often requiring synchronous pumping of external cavity Raman lasers to achieve high (>30%) conversion efficiencies [8–11]. Mode-locked pump sources used in these Raman laser experiments are also rather complex. They usually emit at the repetition rates of several MHz and typical pulse energies vary from sub-nJ (for fs lasers) to sub-µJ (for ps lasers). On the other hand, power amplification (PA) of master oscillation (MO) from passively Q-switched microchip lasers emitting sub-ns pulses at several kHz repetition rate could often be a simpler alternative to mode-locked lasers.

In this report such a MOPA is used as a pump source. The 532 nm MOPA produced 85 ps pulses with up to 500 mW of average power at a repetition rate of 100 kHz with M^2 of <1.88. The MO was a Q-switched 100 µm thick $Nd:YVO_4$ single-frequency microchip laser emitting 10 mW of average power and 100 ps pulses at 1064 nm. The signal was amplified to >1 W average power with a $Nd:YVO_4$ bulk power amplifier and frequency-doubled with a 10 mm long LBO crystal.

Exploiting the high Raman gain in diamond [12, 13], it has been previously demonstrated that near quantum limited conversion efficiencies of 532 nm nanosecond pulses can be achieved in a 2-mm long, monolithic Raman cavity [3]. Such resonators should also be short enough to efficiently convert sub-100 ps pulses by allowing several round trips of the intra-cavity Raman field per pump pulse. Here 85 ps pump pulses are converted to 1st Stokes, 573 nm, emission with conversion efficiency of 36–52% and pulse duration of 39–76 ps in a 0.5 mm long plane–plane monolithic diamond Raman laser.

II. Experimental and Results

A single crystal synthetic diamond sample with 4 mm diameter and 0.5 mm thickness was employed. The diamond was fabricated by Element 6 Ltd. using chemical vapor deposition, and had a birefringence of $<1\times10^{-5}$ and specified absorption coefficient of $<0.01\ cm^{-1}$ at 1064 nm (it is ~2.5 times higher at ~570 nm [12]). Laser mirror coatings were deposited on the diamond to form a plane–plane monolithic diamond Raman laser cavity. The input coupler provided ~82% transmission for the pump at 532 nm, and high reflectivity (HR) for the Raman laser at 573 nm. The output coupler (OC) was highly reflective at 532 nm to enable a double pass of the pump, and partially reflective at 573 nm. A schematic of the setup and

Manuscript submitted XX.YY.ZZZZ. This work was financially supported in part by Academy of Finland (282431); European Research Council (278389, 727738); UK EPSRC (EP/P00041X/1, EP/L015315/1); Fraunhofer UK Research Ltd.; Royal Academy of Engineering; Element 6 (UK) Ltd. Results of modelling are openly available from the University of Strathclyde Pure/ KnowledgeBase at http://dx.doi.org/10.15129/0922b283-e61e-417a-b371-cf4d6e68e097

Jari Nikkinen, Antti Härkönen and Mircea Guina are with the Optoelectronics Research Centre, Tampere University of Technology, Korkeakoulunkatu 3, 33720 Tampere, Finland (e-mail: jari.nikkinen@tut.fi)

Vasili Savitski, Sean Reilly, Łukasz Dziechciarczyk and Alan Kemp are with the Institute of Photonics, Department of Physics, SUPA, University of Strathclyde, 99 George street, Glasgow G1 1RD, UK (e-mail: vasili.savitski@strath.ac.uk)

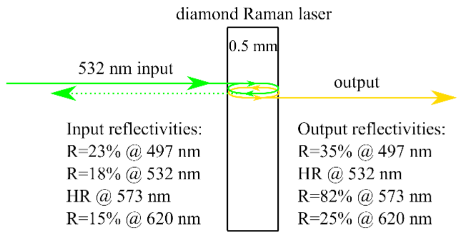

Fig. 1. A schematic presentation of the diamond Raman laser.

coating details are given in Fig. 1. Pump focusing optics of 100, 75, and 50 mm focal length were used, giving calculated pump diameters of ~62 µm, ~47 µm, and ~31 µm, respectively.

The output characteristics of the Raman laser (Fig. 2) were measured as a function of incident 532 nm pump power using a 3W thermal power meter (Ophir Optronics). The highest 1st Stokes output power of 179 mW with conversion efficiency of 47% was achieved with the f=75 mm lens and pump spot diameter of ~47 µm. This conversion efficiency to the 1st Stokes is higher than that reported for 1.5 ns pump pulses in plane-plane configuration (38%) [3]. A slight wedge between the diamond surfaces (which adds losses), differences in coatings and the presence of the 2nd Stokes at high pump powers are the main limiting factors in conversion efficiency. By scaling up the pump spot size (~62 µm) with a f=100 mm lens, 150 mW of 573 nm output power was achieved with 36% conversion efficiency and reduced pulse duration of 39 ps. Up to 16.4 mW of 2nd Stokes average power was obtained in the forward direction with the f=50 mm focusing lens. The 1st anti-Stokes line (497 nm) was present at all pump spot sizes studied; however, the maximum average power was only 2 mW in the forward direction. With the f=50 mm focusing lens some tens to hundreds of µW of 3rd Stokes (676 nm), and 2nd anti-Stokes (466 nm) were observed at high pump powers.

The autocorrelation traces (Fig. 3) were measured with a

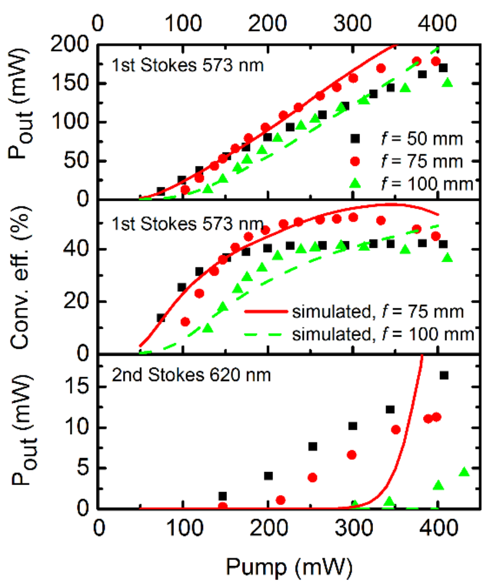

Fig. 2. Top: 1st Stokes output characteristics Middle: Raman conversion efficiency from 532 nm to 573 nm. Bottom: 620 nm output power. All given as a function of incident 532 nm pump power. Pump focusing lenses f = 50 mm, f = 75 mm and f = 100 mm. Simulations: solid and dashed lines.

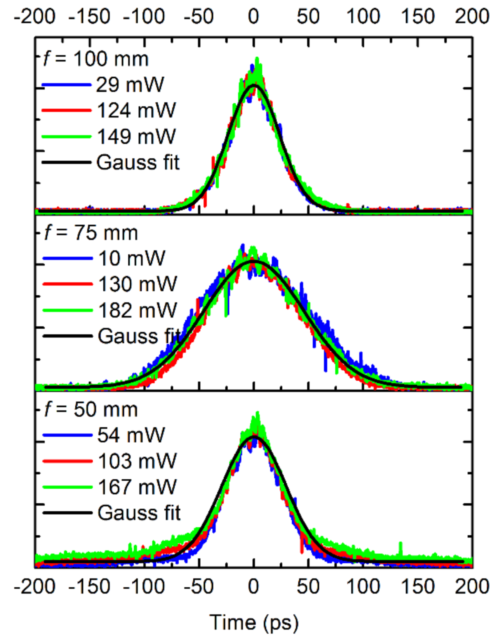

Fig. 3. Autocorrelation traces of 1st Stokes lines obtained with pump focusing lenses having focal distances of 100 mm, 75 mm and 50 mm. Gaussian fits made to highest power traces.

Femtochrome FR-103WS autocorrelator and corresponding pulse durations were calculated using Gaussian fits. The Raman pulse duration remained nearly constant for f=100 mm (36–39 ps) and f=75 mm (65–76 ps) pump focusing lenses, over the range of pump powers used. With the f=50 mm lens, the appearance of significant 2nd Stokes started to deplete the 1st Stokes, causing the pulse shape to distort (Fig. 3).

The typical standard deviation of the average output power fluctuations of the 1st Stokes was <1% over 10 minutes, a value similar to the pump, measured at ~100 mW output power. Pulse-to-pulse energy fluctuations (measured using a 10 MHz Si-photodiode) for the 1st Stokes were <8% at 160 mW output power, and much larger for 2nd Stokes and 1st anti-Stokes. The pulse trains measured with the f=50 mm lens are shown in Fig. 4. The output spectra (Fig. 5) were measured with a Yokogawa AQ6373 spectrum analyzer (0.02 nm resolution). Spectral widths of the Raman output were approximately 0.035 nm, slightly broader than the 0.026 nm spectral width of the pump. The secondary peaks in the spectra (Fig. 5 (b,c)) are separated by ~2.5 cm^{-1} and may be due to Brillouin scattering in diamond [14]. The photograph in Fig. 5(f) was taken when the diamond was tilted by ~2° with respect to the incoming pump beam to better satisfy the phase-matching conditions required for efficient 2nd anti-Stokes conversion [15]. The 1st Stokes output beam consisted of several concentric rings, similar to results in [3]. For that reason no reliable measurements of the M^2 factor of the beam could be made.

Preliminary analysis indicates that Raman gain-guiding may be the major mechanism determining the transverse mode in a plane–plane diamond Raman laser [16], particularly given that the minimum focal length of the thermal lens was calculated to be ~17 m. Further study is currently underway.

The rate equations for the extra-cavity Raman laser

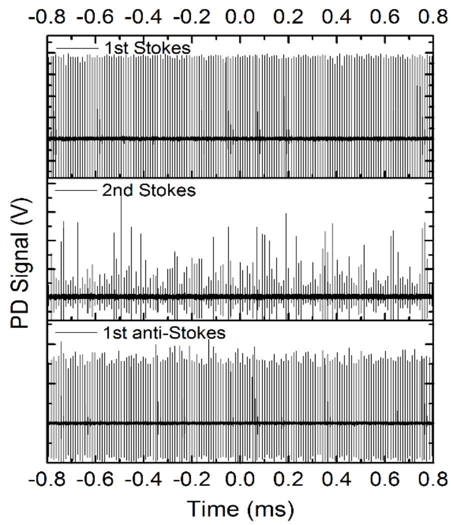

Fig. 4. Photodiode (PD) signal showing pulse trains of the 1st Stokes, 2nd Stokes and 1st anti-Stokes output (f=50 mm).

introduced in [17] were used to simulate the experimental results. The model does not take into account anti-Stokes generation, or overlap of the Raman modes. Therefore, the simulations were carried out only for lenses with f=75 and 100 mm, where the experimentally observed effects of anti-Stokes generation are less pronounced. Simulated output powers and conversion efficiencies include total (backward and forward) Raman components. The fitting parameters in the modeling were the effective Raman gain (g_{eff}) and a dimensionless spontaneous scattering factor (k_{sp}) for the 1st and 2nd Stokes. Effective Raman gain is determined by the overlap factor between the pump and the Raman modes, and by the

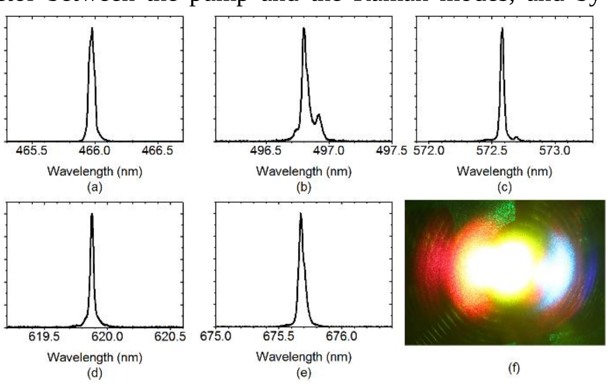

Fig. 5. Output spectra of the diamond Raman laser from 2nd anti-Stokes (a) to 3rd Stokes (e), and a photograph of the laser output beam showing the five wavelengths (f).

linewidth of the pump emission [12, 18]. The results of the modelling presented in Figs. 2 and 6 are for the following parameters: g_{eff1}=26 cm/GW, g_{eff2}=8 cm/GW, $k_{sp1}=3\times10^{-3}$ and $k_{sp2}=10^{-8}$. These effective gain values indicate that the "Raman gain reduction factors" [19] are 0.6 and 0.2 for the 1st and the 2nd Stokes, assuming Raman gain values at 532 nm and 573 nm of ~40 and 39 cm/GW, correspondingly [12]. Higher gain reduction factor for the Raman gain at 573 nm could be due to broader linewidth. It should be noted that experimental data in Fig. 2 do not account for the possible backward propagating 2nd

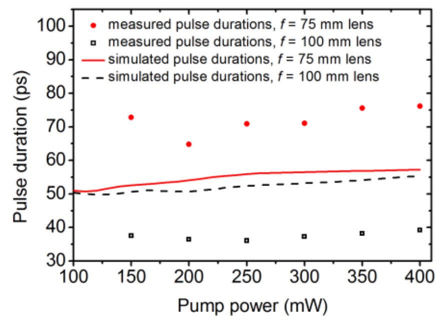

Fig. 6. Measured and simulated pulse durations as a function of the pump power, with pump focusing lenses of f=75 mm and f=100 mm.

Stokes power. The simulated 1st Stokes pulse duration (~55 ps) does not change significantly with the pump power, in accordance with the experimental results (Fig. 6), and was found to be roughly the same for both focusing lenses.

TABLE I
LASER OUTPUT PARAMETERS

		Pump focal length (mm)		
Calculated pump spot		100	75	50
diameter	µm	62	47	31
1st Stokes, 573 nm				
Output power[a]	mW	127	157	162
Max pump conv. eff.	%	40.6	52.1	42.3
Pulse duration[a]	ps	39.2	71.0	~48.9[b]
Threshold	mW	109	83.3	52.7
Slope efficiency	%	73.4	80.6	54.7
2nd Stokes, 620 nm				
Output power[a]	mW	4.4	11.3	16.4
Max pump conv. eff.	%	1.0	2.8	3.6
Pulse duration[a]	ps	-	-	~59[b]
Threshold	mW	302	164	122
Slope efficiency	%	3.2	4.9	5.7
1st anti-Stokes, 497 nm				
Output power[a]	mW	0.22	0.28	1.97
Max pump conv. eff.	%	0.052	0.083	0.49
Threshold	mW	209	82	96
Slope efficiency	%	0.10	0.10	0.64

a) Output power and pulse duration at maximum pump conversion efficiency; b) Pulse shape is not Gaussian.

However, the experimentally observed pulse duration rises from ~40 ps for the f=100 mm lens to ~70 ps for the 75 mm one. This could be due to several factors: a mismatch in overlap of the pump and Stokes signal, difference in spontaneous scattering factor (k_{sp}) for different configurations, influence of the anti-Stokes generation, which could distort and lengthen the 1st Stoke pulse duration. The modelling suggests that the output coupler reflectivity used in our experiment is close to the optimum for maximum conversion efficiency. Decreasing the output coupler reflectivity from 80% to 30% shortens the predicted 1st Stokes pulse duration by a factor of 2, while the conversion efficiency drops by only 7%.

III. Conclusion

In conclusion, we have demonstrated a diamond Raman laser producing 150 mW of 1st Stokes Raman emission at 573 nm with pulse duration of 39 ps and pump conversion efficiency of 36%, at 100 kHz pulse repetition rate. By decreasing the pump spot size, we achieved up to 47% pump conversion efficiency with a maximum 1st Stokes Raman output power of 175 mW yielding 0.18 µJ in pulse energy and pulse duration of 71 ps. For a given pump intensity, the conversion efficiency in the steady-state regime (pump pulse duration >> dephasing time of the Raman crystal [20] (6.8 ps in diamond [10])), is mainly determined by the number of roundtrips of the Stokes during the pump pulse and the reflectivity of the output mirror [21]. Analysis [21] shows that conversion efficiency saturates after about 15 round-trips if the output coupler reflectivity is optimised. In [3] the conversion efficiency to the 1st Stokes in the plane-plane cavity configuration was 38% with 1.5 ns pump pulse duration and the diamond (resonator) length of 1.6 mm. The number of round-trips of the Stokes emission in the cavity during the FWHM pump pulse duration in that case was 58. In our case, the number of round-trips is only 10, but the conversion efficiency to the 1st Stokes is even higher (52%) due to more optimal reflectivity of the output coupler. Even so, this short gain period will limit the conversion efficiency. When considering even shorter pump pulses (10–20 ps) for monolithic Raman lasers, one has to consider two additional factors: i) Raman scattering will be in the quasi-steady-state regime with reduced conversion efficiency [20] (e.g. in [10] it was 25.6% under synchronous pumping of diamond Raman laser); ii) the thickness of diamond required for 10–15 round-trips with ~20 ps pump pulses is ~0.1 mm, making fabrication challenging. The conversion efficiency is likely to be improved by using microlens structures etched into the diamond surface [3].

By reducing the pump spot size, we achieved 16.4 mW of 2nd Stokes Raman emission at 620 nm, while the corresponding 1st Stokes emission had 162 mW power with 49 ps pulse duration. By coating optimization it should be also possible to increase the output power of higher order Stokes lines, if required. In addition, monolithic resonators are equally applicable to other Raman crystals, and Raman conversion in plane-plane cavity with barium nitrate crystal was recently demonstrated [22].

Overall, we believe that the concept of a SESAM Q-switched microchip pump source, in combination with a monolithic diamond Raman laser, offers an interesting alternative for generation of picosecond visible pulses outside common 532/355/266 nm wavelengths. The main advantages are its simple design and unique combination of output parameters, including short pulse duration, high pulse intensity, low repetition rate and narrow spectrum. In our view, the system defines a new frontier in terms of simplicity and parameters attained, making such a picosecond yellow pulsed source appealing to a wide range of applications.

References

[1] R. Carriles, D. N. Schafer, K. E. Sheetz, J. J. Field, R. Cisek, V. Barzda, A. W. Sylvester, and J. A. Squier, “Invited Review Article: Imaging techniques for harmonic and multiphoton absorption fluorescence microscopy,” *Rev. Sci. Instrum.* 80, p. 081101 (2009).

[2] I. Friel, S. L. Geoghegan, D. J. Twitchen, and G. A. Scarsbrook, “Development of high quality single crystal diamond for novel laser applications,” *Proc. SPIE*, 7838, pp. 783819–1 (2010).

[3] S. Reilly, V. G. Savitski, H. Liu, E. Gu, M. D. Dawson, and A. J. Kemp, “Monolithic diamond Raman laser,” *Opt. Lett.*, 40(6), pp. 930–933 (2015).

[4] V. G. Savitski, I. Friel, J. E. Hastie, M. D. Dawson, D. Burns, and A. J. Kemp, “Characterization of single-crystal synthetic diamond for multi-watt continuous-wave Raman lasers,” *IEEE J. Quantum Electron.* , 48(3), pp. 328–337 (2012).

[5] W. Lubeigt, G. M. Bonner, J. E. Hastie, M. D. Dawson, D. Burns, and A. J. Kemp, “An intra-cavity Raman laser using synthetic single-crystal diamond,” *Opt. Express*, 18(16), 16765–16770 (2010).

[6] J.-P. M. Feve, K. E. Shortoff, M. J. Bohn, and J. K. Brasseur, “High average power diamond Raman laser,” *Opt. Express*, 19(2), pp. 913–922 (2011).

[7] O. Kitzler, A. McKay, and R. P. Mildren, “Continuous-wave wavelength conversion for high-power applications using an external cavity diamond Raman laser,” *Opt. Lett*., 37(14), pp. 2790–2792 (2012).

[8] P. Černý, H. Jelinková, T. T. Basiev, and P. G. Zverev, “Highly efficient picosecond Raman generators based on the $BaWO_4$ crystal in the near infrared, visible, and ultraviolet,” *IEEE J. Quantum Electron.*, 38(11), pp. 1471–1478 (2002).

[9] M. Murtagh, J. Lin, R. P. Mildren, and D. J. Spence, “Ti:sapphire-pumped diamond Raman laser with sub-100-fs pulse duration,” *Opt. Lett.*, 39(10), pp. 2–5 (2014).

[10] D. J. Spence, E. Granados, and R. P. Mildren, “Mode-locked picosecond diamond Raman laser,” *Opt. Lett.*, 35(4), pp. 556–558 (2010).

[11] P. G. Zverev, J. T. Murray, R. C. Powell, R. J. Reeves, and T. T. Basiev, “Stimulated Raman scattering of picosecond pulses in barium nitrate crystals,” *Opt. Commun.*, 97(1–2), pp. 59–64 (1993).

[12] V. G. Savitski, S. Reilly, and A. J. Kemp, “Steady-state Raman gain in diamond as a function of pump wavelength,” *IEEE J. Quantum Electron.*, 49(2), pp. 218–223 (2013).

[13] A. Sabella, D. Spence, and R. Mildren, “Pump-probe measurements of the Raman gain coefficient in crystals using multi-longitudinal-mode beams,” *IEEE J. Quantum Electron.*, 51(12), p. 1000108 (2015).

[14] R. J. Williams, J. Nold, M. Strecker, O. Kitzler, A. McKay, T. Schreiber and R. P. Mildren, “Efficient Raman frequency conversion of high-power fiber lasers in diamond” *Laser & Photonics Reviews*, **9**, 405–411, (2015).

[15] C. Wang, X. Zhang, Q. Wang, Z. Cong, Z. Liu, W. Wei, W. Wang, Z. Wu, Y. Zhang, L. Li, X. Chen, P. Li, H. Zhang, and S. Ding, “Extracavity pumped $BaWO_4$ anti-Stokes Raman laser,” *Opt. Express* 21, pp. 26014–26026 (2013).

[16] V. G. Savitski, S. Reilly, and A. J. Kemp, “Yellow-orange emission from a plane-plane monolithic diamond Raman laser,” in 2015 European Conference on Lasers and Electro-Optics, Munich, 2015, p. CA_8_4.

[17] S. Ding, X. Zhang, Q. Wang, F. Su, S. Li, S. Fan, S. Zhang, J. Chang, S. Wang, and Y. Liu, “Theoretical models for the extracavity Raman laser with crystalline Raman medium”, *Appl. Phys. B* 85, pp. 89–95, (2006).

[18] A. Sabella, J. A. Piper, and R. P. Mildren, "Efficient conversion of a 1.064 µm Nd:YAG laser to the eye-safe region using a diamond Raman laser," *Opt. Express* 19, pp. 23554–23560 (2011).

[19] D. C. Parrotta, A. J. Kemp, M. D. Dawson, and J. E. Hastie, "Multiwatt, continuous-wave, tunable diamond Raman laser with intracavity frequency-doubling to the visible region," *IEEE J. Sel. Top. Quantum Electron.* 19, pp. 1400108–1400108 (2013).

[20] P. Černý and H. Jelínková, “Near-quantum-limit efficiency of picosecond stimulated Raman scattering in $BaWO_4$ crystal”, *Optics Letters* 27, pp. 360–362, (2002).

[21] A. Penzkofer, A. Laubereau, and W. Kaiser, “High-intensity Raman interactions”, *Prog. in Quantum Electr.* 6, pp. 56–140, (1979).

[22] R. V. Chulkov, V. Y. Markevich, A. Y. Alyamani, E. A. Cheshev, and V. A. Orlovich, “Cavity length matching and optical resonances in a Raman laser with the multimode pump source”, *Opt. Lett.* 42, pp. 4824–4827 (2017).